of declining rate constants with increasing distance. While we might expect such a trend, the apparent lack of any direct correlation most presumably arises from the pecularities of each protein system.

Since most literature examples of LRET in proteins involve two metal redox sites, it may not be recognized generally that there are a number of non-metal sites on proteins that, given the proper reagent, can be reduced or oxidized.[15] Moreover, the radicals so formed can participate in intramolecular electron-transfer reactions.[9,10] Hence, it is imperative to verify both the electron donor and acceptor in a protein intramolecular redox reaction. In the experiments we report here, we have measured spectral changes associated with both the disulfide radical anion and the α subunit heme group. Moreover, since we have found that $CO_2^{\bullet-}$ reduces the heme group in Fe(III)-α-Hb with no attached disulfide and predominantly the disulfide of Fe(III)-α-Hb-SSR, unwanted side reactions due to "contaminating" radical reduction at other protein sites most presumably do not occur in this system.

Acknowledgment. This work was supported by NIH Grant GM-35718 and by Grant No. 85-00217 from the United States-Israel Binational Science Foundation (BSF), Jerusalem, Israel.

Registry No. $CO_2^{\bullet-}$, 2564-86-5; heme, 14875-96-8; cysteine, 52-90-4.

Oxoferryl Complexes of the Halogenated (Porphinato)iron Catalyst: (Tetrakis(2,6-dichlorophenyl)porphinato)iron

A. Gold,* K. Jayaraj, P. Doppelt, R. Weiss,* G. Chottard,* E. Bill, X. Ding, and A. X. Trautwein*

Contribution from the Department of Environmental Sciences and Engineering, University of North Carolina at Chapel Hill, Chapel Hill, North Carolina 27514, the Institut Le Bel, Université Louis Pasteur, 67070 Strasbourg, France, the Université Pierre et Marie Curie, 75230 Paris Cedex 05, France, and the Institut für Physik, Medizinische Universität, D-2400 Lübeck 1, FRG. *Received January 26, 1988*

Abstract: Oxidation of (hydroxo)(tetrakis(2,6-dichlorophenyl)porphinato)iron(III) [TPP(2,6-Cl)Fe^{III}OH] by *m*-chloroperoxybenzoic acid (mCPBA) in THF or DMF yields the THF and DMF adducts of the oxoferryl complex TPP(2,6-Cl)Fe^{IV}=O. Addition of 10-fold molar excess of 1-methylimidazole (1-MeIm) to the THF adduct gives the corresponding 1-MeIm complex. ^{1}H NMR of the DMF-d_7 adduct (200 MHz, DMF-d_7, −50 °C) shows proton resonances consistent with an oxoferryl S = 1 structure: 14 ppm (pyrrole H), 4.01 ppm (phenyl *m*- and *p*-H) in a ratio of 2:3. The UV-vis spectra (−40 °C) of the red solutions show the band at ~550 nm which is typical of the ferryl oxidation state: (THF) TPP(2,6-Cl)Fe^{IV}=O, λ_{max}($\epsilon \times 10^{-3}$) 417 (169.5), 551 (10.6), 622 (3.4), 653 (1.4) nm; (DMF) TPP(2,6-Cl)Fe^{IV}=O, λ_{max} ($\epsilon \times 10^{-3}$) 419 (157.6), 554 (11.1), 632 (3.5) nm; (1-MeIm) TPP(2,6-Cl)Fe^{IV}=O, λ_{max} ($\epsilon \times 10^{-3}$) 421 (157.5), 561 (13.2), 624 (3.3), 661 (1.8) nm. Resonance Raman bands in the region of the Fe=O stretch provide support for the oxoferryl structure with frequencies that correlate inversely with the strength of the sixth axial ligand: THF (841 cm^{-1}) < DMF (829 cm^{-1}) < 1-MeIm (818 cm^{-1}). The Mössbauer spectra, similar to those of other ferryl S = 1 complexes, establish the ferryl oxidation state of iron. While quadrupole splittings vary inversely with axial ligand strength (THF (2.08 mm s^{-1}) < DMF (1.81 mm s^{-1}) < 1-MeIm (1.35 mm s^{-1})), isomer shifts are essentially constant. Resonance Raman and Mössbauer data are rationalized by a rearrangement of bonding electron density from Fe $3d_{x^2-y^2}$ to $3d_{z^2}$ with increasing axial ligand bonding. The Fe=O bond weakens, decreasing $\nu_{Fe=O}$, and the axial electric field gradient decreases, giving smaller quadrupole splitting. However, little net change in electron density at Fe results in constant δ.

Chloro(tetrakis(2,6-dichlorophenyl)porphinato)iron(III) [TPP(2,6-Cl)FeCl] is frequently employed as a monooxygen transfer catalyst because of the resistance of the porphyrin ring to oxidative degradation and the high reactivity of the intermediate compound I analogue. Hydroxylations of alkanes[1] and stereospecific epoxidations of olefins[2-4] have been described and the high number of turnovers achievable with this catalyst has also enabled the "suicide" formation of N-alkylated porphyrin complexes to be extensively studied.[5-8] Despite interest in the catalytic properties of TPP(2,6-Cl)Fe^{III} and a number of reports in which reactions were carefully monitored by UV-vis spectroscopy,[1,5,7] no complex with iron in the ferryl oxidation state has been directly observed or characterized. Nevertheless, physicochemical data on high-valent complexes should prove important in understanding the chemistry of the one- and two-electron oxidized species of this useful catalyst as well as other bifacially hindered (porphinato)iron complexes currently used to probe mechanisms of biological oxidations. Hence we have attempted to develop conditions under which observable high-valent complexes of iron 2,6-dichlorophenyl porphyrin can be generated and studied. We report here the characterization of the oxoferryl compound II analogue, TPP(2,6-Cl)Fe^{IV}=O, generated by the oxidation of the hydroxo complex with mCPBA and stabilized by axially ligated dimethylformamide (DMF), tetrahydrofuran (THF), or 1-methylimidazole (1-MeIm). Observation of transients in UV-vis and ^{1}H NMR spectra during the oxidation reactions has provided insights into the pathway leading to the oxoferryl complex.

Results

Oxidation of TPP(2,6-Cl)FeOH in DMF and THF. Oxidation of TPP(2,6-Cl)FeOH with mCPBA in DMF-d_7 at −50 °C yielded a deep red solution with an ^{1}H NMR spectrum consisting of

(1) Traylor, P. S.; Dolphin, D.; Traylor, T. G. *J. Chem. Soc., Chem. Commun.* **1984**, 279.
(2) Traylor, T. G.; Marsters, J. C.; Nakano, T. *J. Am. Chem. Soc.* **1985**, *107*, 5537.
(3) Traylor, T. G.; Nakano, T.; Dunlap, B. E.; Traylor, P. S.; Dolphin, D. *J. Am. Chem. Soc.* **1986**, *108*, 2782.
(4) Traylor, T. G.; Miksztal, A. R. *J. Am. Chem. Soc.* **1987**, *109*, 2770.
(5) Mashiko, T.; Dolphin, D.; Nakano, T.; Traylor, T. G. *J. Am. Chem. Soc.* **1985**, *107*, 3735.
(6) Collman, J. P.; Hampton, P. D.; Brauman, J. I. *J. Am. Chem. Soc.* **1986**, *108*, 7861.
(7) Traylor, T. G.; Nakano, T.; Miksztal, A. R.; Dunlap, B. E. *J. Am. Chem. Soc.* **1987**, *109*, 3625.
(8) Artaud, I.; Devocelle, L.; Battioni, J. P.; Girault, J.-P.; Mansuy, D. *J. Am. Chem. Soc.* **1987**, *109*, 3782.

0002-7863/88/1510-5756$01.50/0

Table I. ^{1}H NMR Shifts of High-Valent Iron Tetraarylpoprhyrin Complexes

compd	solvent	temp (°C)	proton shifts (ppm) py-H	ortho	meta	para	ref
(1-MeIm)·(TPP)Fe^{IV}=O	tol-d_8	−80	5.05	9.2, ...	7.9	7.9	9
(TMP)Fe^{IV}=O	tol-d_8	−70	8.4	3.3,[a] ...	6.4, 6.6	2.6[a]	10, 11
(1-MeIm)·(TMP)Fe^{IV}=O	tol-d_8	−30	4.6	3.2,[a] 1.6[a]	7.4	2.67[a]	11
(THF)·[TP(piv)P]Fe^{IV}=O	THF-d_8	−50	7.2	12.9	9.3, 8.7	7.7	12
2	DMF-d_7	−50	14.1		4.01	4.01	*b*
(TMP)$Fe^{IV}(OCH_3)_2$	CD_2Cl_2/CD_3OD	−78	−37.5	2.4[a]	7.72	2.86[a]	13, 14
[(TMP)Fe^{IV}=O]$^+Cl^-$	tol-d_8/CD_3OD	−70	−16	25.6,[a] 24.4[a]	63.6, 62.4	11[a]	10
[(TMP)Fe^{IV}=O]$^+Cl^-$	CD_2Cl_2/CD_3OD	−77	−27	26,[a] 24[a]	68	11.1[a]	15
[TPP(2,6-Cl)Fe^{IV}=O]$^+OH^-$	CD_2Cl_2	−60	−33.8		38.9, 38.0	...	*b*

[a] Methyl resonance. [b] This work.

Table II. Electronic Spectra of High-Valent Iron Porphyrin Complexes

compd	solvent	temp (°C)	λ_{max} ($\epsilon \times 10^{-3}$) (nm)	ref
(1-MeIm)·(TPP)Fe^{IV}=O[a]	tol	−90	425 (195), 555 (15), 590 (8.6)	9
(TMP)Fe^{IV}=O	CH_2Cl_2/0.05 M TBAP	−40	414 (102), 545 (12.7)	18
(THF)·[TP(piv)P]Fe^{IV}=O	THF	−70	419, 550	12
(1-MeIm)·[TP(piv)P]Fe^{IV}=O	THF	−70	426, 560	12
1	THF	−50	417 (169.5), 551 (10.6), 622 (3.4), 653 (1.4)	*b*
2	DMF	−50	419 (157.6), 554 (11.1), 632 (3.5)	*b*
3	THF	−50	421 (157.5), 561 (13.2), 624 (3.3), 661 (1.8)	*b*
4	CH_2Cl_2	−60	416 (138.4), 552 (8.6)	*b*
(TMP)$Fe^{IV}(OCH_3)_2$	CH_2Cl_2/MeOH	−38	425.5 (119.2), 546 (16.3), 575 (7.7)	13, 14
[(TMP)Fe^{IV}=O]$^+Cl^-$	CH_2Cl_2/MeOH	−77	406, 645	15
5	CD_2Cl_2	−60	408 (31.7), 688 (2.4)	*b*

[a] λ_{max} estimated from the trace presented in ref 9. [b] This work.

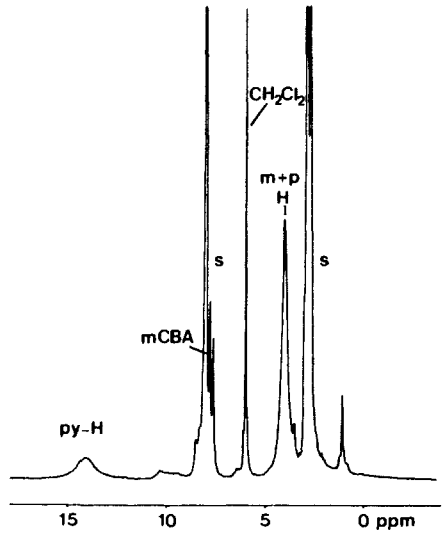

Figure 1. ^{1}H NMR spectrum (200 MHz, DMF-d_7, −50 °C). Assignment of proton resonances: py-H, pyrrole; *m*+*p*-H, phenyl meta and para protons; mCBA, *m*-chlorobenzoic acid; S, residual solvent protons.

broadened resonances at 14.1 and 4.01 ppm downfield from TMS and having relative areas in the ratio 2:3, respectively (Figure 1). The low-field peak was assigned as the pyrrole β-proton signal on the basis of its integrated area and Curie law dependence, extrapolating to 10 ppm at infinite temperature, close to the diamagnetic shift for porphyrin pyrrole β-protons. The resonances in Figure 1 occur at shifts within the range expected[9-15] for an oxoferryl complex (Table I); in particular, the small hyperfine

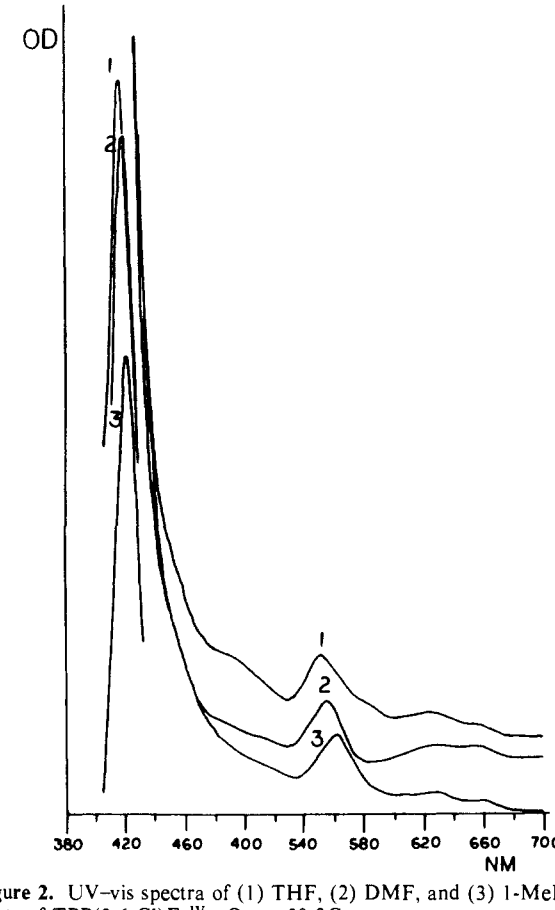

Figure 2. UV–vis spectra of (1) THF, (2) DMF, and (3) 1-MeIm adducts of TPP(2,6-Cl)Fe^{IV}=O at −50 °C.

shifts observed are typical of complexes containing the $(Fe^{IV}=O)^{2+}$ unit in which unpaired spin resides principally on the oxoferryl group.[16,17] The pyrrole β-proton resonance of a bis hydroxo ferryl compound would be expected to appear well upfield of TMS

(9) Chin, D.-H.; Balch, A. L.; LaMar, G. N. *J. Am. Chem. Soc.* **1980**, *102*, 1446.
(10) Balch, A. L.; Latos-Grazynski, L.; Renner, M. W. *J. Am. Chem. Soc.* **1985**, *107*, 2983.
(11) Balch, A. L.; Chan, Y.-W.; Cheng, R. J.; LaMar, G. N.; Latos-Grazynski, L.; Renner, M. W. *J. Am. Chem. Soc.* **1984**, *106*, 7779.
(12) Schappacher, M.; Weiss, R.; Montiel-Montoya, R.; Trautwein, A.; Tabard, A. *J. Am. Chem. Soc.* **1985**, *107*, 3736.
(13) Groves, J. T.; Quinn, R.; McMurry, T. J.; Nakamura, M.; Lang, G.; Boso, B. *J. Am. Chem. Soc.* **1985**, *107*, 354.
(14) Groves, J. T.; Quinn, R.; McMurry, T. J.; Lang, G.; Boso, B. *J. Chem. Soc., Chem. Commun* **1984**, 1455.
(15) Groves, J. T.; Haushalter, R. C.; Nakamura, M.; Nemo, T. E.; Evans, B. J. *J. Am. Chem. Soc.* **1981**, *103*, 2884.
(16) Loew, G. H.; Herman, Z. S. *J. Am. Chem. Soc.* **1980**, *102*, 6175.
(17) Hanson, L. K.; Chang, C. K.; Davis, M. S.; Fajer, J. *J. Am. Chem. Soc.* **1981**, *103*, 663.

Table III. Mössbauer Effect Spectra of Ferryl Complexes in the Absence of an Applied Magnetic Field

compd	temp (K)	matrix	δ (mm s^{-1})	ΔE_q (mm s^{-1})	Γ (mm s^{-1})	ref
(1-MeIm)·(TPP)Fe^{IV}=O	4.2	solid	0.12	1.24		19
(1-MeIm)·(TPP)Fe^{IV}=O	4.2	tol	0.11	1.26		19
(pyridine)·(TPP)Fe^{IV}=O	4.2	tol	0.10	1.56		19
(THF)·TP(piv)Fe^{IV}=O	4.2	THF	0.120	2.200	0.414	12
(1-MeIm)·TP(piv)Fe^{IV}=O	4.2	THF	0.109	1.372	0.315	12
(TMP)Fe^{IV}=O	?	tol (?)	0.04	2.3		18
1	4.2	THF	0.09	2.08	0.32	*a*
2	4.2	DMF	0.09	1.81	0.37	*a*
3	4.2	THF	0.07	1.35	0.29	*a*
(TMP)Fe^{IV}(OCH$_3$)$_2$	4.2	tol	−0.022	2.17		13, 14

[a] This work.

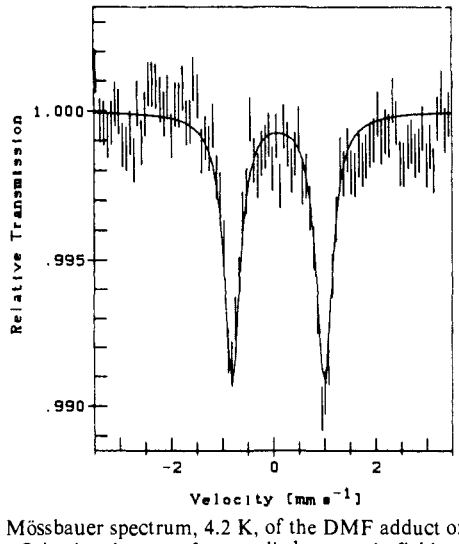

Figure 3. Mössbauer spectrum, 4.2 K, of the DMF adduct of TPP(2,6-Cl)^{57}Fe^{IV}=O in the absence of an applied magnetic field.

(Table I), and a μ-peroxo complex, the only possible species with a pyrrole proton resonance within the region of the observed signal,[11] can be definitively ruled out by UV–vis and Mössbauer data described below.

The electronic spectra (Figure 2) of the complexes generated from mCPBA oxidation of TPP(2,6-Cl)FeOH in THF or DMF displayed bands characteristic[9,12,13-15,18] of ferryl complexes (Table II). A red shift of the Soret and β-bands relative to the positions in THF is evident in the more strongly coordinating DMF solvent, and addition of a 10-fold molar excess of the yet stronger axial ligand, 1-MeIm, to a THF solution of the oxidized complex causes the largest effect (Figure 2). A similar correlation of band position with axial ligand strength has been reported for hexacoordinated oxoferryl "picket fence" porphyrins[12] and implies that the traces in Figure 2 represent the THF, DMF, and 1-MeIm adducts of TPP(2,6-Cl)Fe^{IV}=O (compounds **1**–**3**, respectively).

The isomer shifts of the Mössbauer spectra of the oxidized ^{57}Fe-enriched complex at 4.2 K in frozen DMF (Figure 3) and THF and in THF after the addition of 1-MeIm confirm the ferryl oxidation state of iron in all three adducts. Comparison of Mössbauer parameters of **1**–**3** with those reported[12-14,18-22] for other known S = 1 ferryl compounds (Table III) indicates that they lie within the range expected for the S = 1 spin state. As in the case of the major bands in the electronic spectra, the quadrupole splittings of the Mössbauer spectra also show consistent variation with the strength of axial ligand coordination, ΔE_q decreasing with increasing strength of the axial ligand. A parallel trend is evident in Table III for the THF and 1-MeIm adducts of the oxoferryl

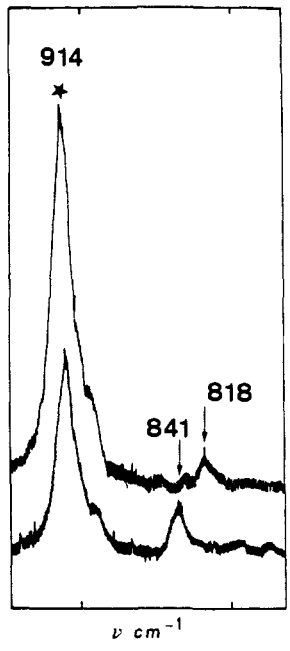

Figure 4. Resonance Raman spectra of THF (lower) and 1-MeIm (upper) adducts of TPP(2,6-Cl)Fe^{IV}=O: static cell; −50 °C; incident light 457.9 nm, 15 mW. Solvent peak is denoted by a star.

Table IV. (Fe^{IV}=O) Stretching Frequencies of Oxoferryl *meso*-Tetraarylporphyrin Complexes

compd	$\nu_{Fe^{IV}=O}$ (cm^{-1})	ref
(TPP)Fe^{IV}=O	852	26, 27
(1-MeIm)·(TPP)Fe^{IV}=O	820	28
(TMP)Fe^{IV}=O	843	29
(THF)·[TP(piv)P]Fe^{IV}=O	829	25
(1-MeIm)·[TP(Piv)P]Fe^{IV}=O	807	25
1	841	*a*
2	828	*a*
3	818	*a*

[a] This work.

picket fence complexes[12] and the pyridine and 1-MeIm adducts[19] of (TPP)Fe^{IV}=O.

Resonance Raman spectra of **1**–**3** exhibit vibrational patterns typical of (tetraarylporphinato)iron in the high-frequency region, with the oxidation state marker band ν_4 located[23] at 1370 cm^{-1}, shifted from 1363 cm^{-1} in the hydroxo ferric complex. In the usually sparse frequency region from 650 to 850 cm^{-1}, a band is observed at 841 cm^{-1} in THF and 829 cm^{-1} in DMF. On addition of 1-MeIm to the THF solution, the band shifts to 818 cm^{-1} (Figure 4). Comparison with previous work on the THF and 1-MeIm adducts of the picket fence complexes[24] as well as other oxoferryl complexes[25-28] (Table IV) allows assignment of bands

(18) Groves, J. T.; Gilbert, J. A. *Inorg. Chem.* **1986**, *25*, 123.
(19) Simonneaux, G.; Scholz, W. F.; Reed, C. A.; Lang, G. *Biochim. Biophys. Acta* **1982**, *716*, 1.
(20) Harami, T.; Maeda, Y.; Morita, Y.; Trautwein, A. X.; Gonser, U. *J. Chem. Phys.* **1977**, *67*, 1164.
(21) Lang, G.; Spartalian, K.; Yonetani, Y. *Biochim. Biophys. Acta* **1976**, *451*, 250.
(22) Schulz, C.; Chiang, R.; Debrunner, P. G. *J. Phys.* **1979**, *40*, C2, 334.
(23) The numbering of the resonance Raman porphyrin bands follows that given by: Abe, M.; Kitagawa, T.; Kiogoku, Y. *J. Chem. Phys.* **1978**, *69*, 4516.
(24) Schappacher, M.; Chottard, G.; Weiss, R. *J. Chem. Soc., Chem. Commun.* **1986**, 93.

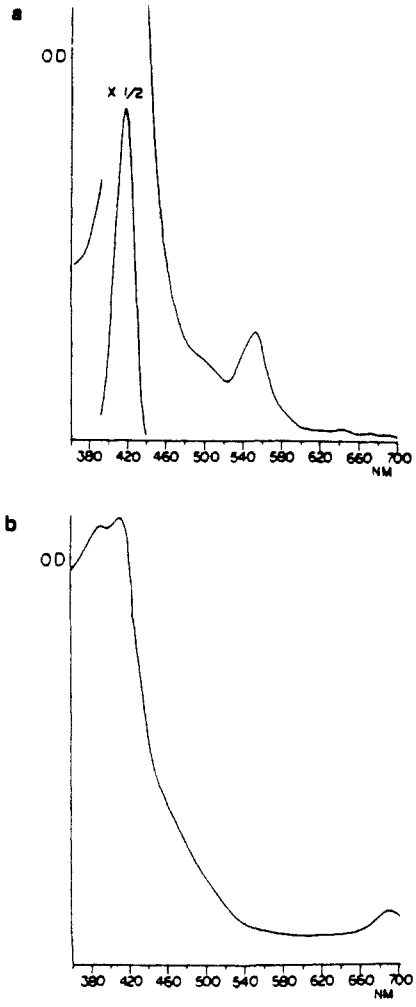

Figure 5. (a) UV–vis spectrum (−60 °C) of oxidized complex obtained from TPP(2,6-Cl)FeOH in methylene chloride containing 0.1% ethanol preservative. (b) UV–vis spectrum (−60 °C) of green transient **5** obtained immediately on addition of mCPBA to TPP(2,6-Cl)FeOH in methylene-d_2 chloride.

in this region to the Fe^{IV}=O stretching vibration. Examination of Table IV for effects of axial ligation on $\nu_{Fe^{IV}=O}$ reveals a regular variation with coordination strength, as observed in electronic and Mössbauer spectra. In the resonance Raman spectra, an increase in axial ligand strength is accompanied by a decrease in the Fe^{IV}=O stretching frequency.

The oxoferryl complex generated in DMF shows exceptional stability. At −5 °C over a period of 2 h, the β-band, the most sensitive marker for the oxoferryl species in the electronic spectrum, decreased by only 5% in intensity. The frozen solution recovered from the apparatus in which Mössbauer samples were generated could be thawed and scanned by UV–vis spectrophotometry in a cuvette at ambient temperature.

Oxidation of TPP(2,6-Cl)FeOH in Methylene Chloride. In attempts to generate a pentacoordinate oxoferryl complex, TPP(2,6-Cl)FeOH was oxidized in methylene chloride solution. In reagent grade solvent containing 0.1% ethanol as preservative, a red complex having an electronic spectrum similar to the THF adduct of the oxoferryl complex formed immediately on mixing with mCPBA at −60 °C (Figure 5). On the basis of the location of the Soret and β-bands (Table II) and the presence of a ca. 9-fold

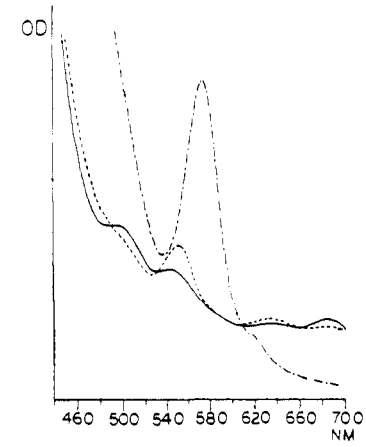

Figure 6. Time dependence of the UV–vis spectrum obtained on oxidation of TPP(2,6-Cl)FeOH in dried, distilled methylene chloride: (···) starting hydroxo complex; (—) immediately after addition of mCPBA; (---) after ~2 min.

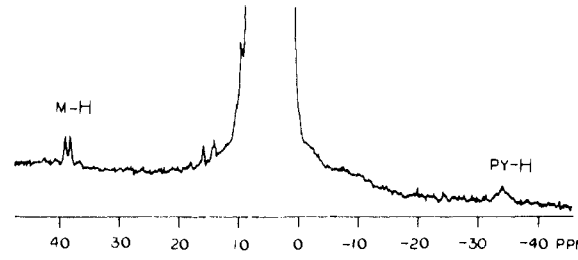

Figure 7. ^{1}H NMR spectrum (200 MHz, methylene-d_2 chloride, −60 °C) of green transient obtained immediately after oxidation of TPP(2,6-Cl)FeOH. Resonances at −33.8 ppm and 38.9, 38.0 ppm are tentatively assigned to the pyrrole and phenyl meta protons, respectively, of an oxoferryl porphyrin cation radical complex (**5**). The resonances at 15.8 and 14.0 ppm are assigned to a high-spin ferric complex and increase in intensity with time at the expense of the set of signals assigned to **5**.

molar excess of ethanol in the reaction solution, the complex may reasonably be assumed to be the ethanol adduct of TPP(2,6-Cl)Fe^{IV}=O (**4**). In carefully dried, distilled methylene chloride, the oxidation generated an initial green transient (**5**) which rapidly decayed (within the time required for a repeat scan, ~2 min) to an oxoferryl complex (Figure 6) and then to a mixture of ferric complexes. In methylene-d_2 chloride the green species persists for a period sufficient to accumulate UV–vis or ^{1}H NMR spectra and decays to a mixture of ferric complexes without passing through an oxoferryl intermediate. The UV–vis trace of the green complex (Figure 5) displays the characteristics reported[15,29] for the two-electron oxidized oxoferryl porphyrin cation radicals of iron tetramesityl porphyrin (Table II). The features of the ^{1}H NMR spectrum (Figure 7) are also consistent with this structural assignment, having a broad singlet upfield of TMS in the region expected for the pyrrole β-proton resonance and two signals downfield, separated by 0.9 ppm, consistent with phenyl *m*-H resonances, although occurring at higher field than reported for the compound I analogue of iron tetramesityl porphyrin from mCPBA oxidation of (TMP)FeCl in either methylene chloride/methanol 4:1[15] or toluene/methanol 4:1[10] (Table I). The phenyl *p*-H signal would be expected to lie within the envelope of peaks between 0 and 10 ppm and is not identified. Larger hyperfine shifts of the porphyrin proton resonances are associated with 2-electron oxidized complexes and are ascribed to an oxoferryl porphyrin cation radical electronic structure in which the second electron has been abstracted from the porphyrin ring, resulting in high unpaired π-spin density in the porphyrin HOMO. Although intermediate-spin iron(III) porphyrin cation radical[13] or bis hydroxo ferryl porphyrin[13,14] structures for the transient have not been rigorously ruled out on the basis of the data presented,

(25) Bajdor, K.; Nakamoto, K. *J. Am. Chem. Soc.* **1984**, *106*, 3045.
(26) Proniewicz, J. M.; Bajdor, K.; Nakamoto, K. *J. Phys. Chem.* **1986**, *90*, 1760.
(27) Kean, R. T.; Oertling, E. A.; Babcock, G. T. *J. Am. Chem. Soc.* **1987**, *109*, 2185.
(28) Hashimoto, S.; Tatsuno, Y.; Kitagawa, T. In *Proceedings of the Tenth International Conference on Raman Spectroscopy*; Petiolas, W. L., Hudson, B., Eds.; University of Oregon: Eugene, OR, 1986; pp 1–29.
(29) Groves, J. T.; Watanabe, Y. *J. Am. Chem. Soc.* **1986**, *108*, 507.

the electronic spectrum argues strongly against either of these two assignments. Therefore, on the basis of the UV–vis and ^{1}H NMR spectra, the green complex **5** is tentatively identified as [TPP-(2,6-Cl)Fe^{IV}=O]$^+$OH$^-$.

Discussion

The array of spectroscopic data by which complexes **1–3** have been characterized are completely consistent with structural assignments as the THF, DMF, and 1-MeIm adducts of TPP-(2,6-Cl)Fe^{IV}=O. The changes observed in spectral parameters of the different adducts comprise a self-consistent set of observations that can be readily interpreted according to current understanding of structure and bonding in oxoferryl complexes, further supporting the proposed structures. In the series of axial ligands with increasing affinities for the porphyrin iron (THF < DMF < 1-MeIm), the effect of strengthening ligation at the sixth axial position is to weaken Fe^{IV}=O bonding interaction, either by a trans effect or by movement of the iron atom toward the porphyrin plane. By this rationale, $\nu_{Fe^{IV}=O}$ should decrease in the series **1** > **2** > **3**, as observed. Table IV shows that $\nu_{Fe^{IV}=O}$ also decreases as predicted when 1-MeIm is substituted as the axial ligand of (TPP)Fe^{IV}=O and [TP(piv)P]Fe^{IV}=O.

Quadrupole splittings decrease with increasing axial ligand strength in the series **1** > **2** > **3** and parallel trends are observed in Table III for the splittings of the THF and 1-MeIm adducts of [TP(piv)P]Fe^{IV}=O and the pyridine and 1-MeIm adducts of (TPP)Fe^{IV}=O. However, the isomer shifts of these seven complexes do not vary appreciably and do not exhibit a trend toward a linear $\Delta E_q - \delta$ relation proposed by Groves et al.[13] for bis methoxy ferryl tetramesityl porphyrin and a number of other oxoferryl complexes. A simple model explains these observations: Fe $3d_{z^2}$ bonding electron density increases with the increase of bond strength of the sixth axial ligand at the expense of bonding electron density in Fe $3d_{x^2-y^2}$. As a consequence, the (positive) electric field gradient becomes smaller while the rearrangement of 3d charge from $3d_{x^2-y^2}$ to $3d_{z^2}$, without changing the total 3d charge significantly, results in constant electron density $\rho(0)$ at iron and therefore unchanged δ.

The transients observed during the oxidation of TPP(2,6-Cl)-FeOH in methylene chloride strongly support a reaction pathway involving initial 2-electron oxidation to an oxoferryl porphyrin cation radical followed by one-electron reduction via hydrogen atom abstraction. Hence, facile abstraction of the alcoholic hydroxyl hydrogen[30] in reagent grade methylene chloride yields the oxoferryl complex without observable intermediates. With dried, distilled methylene chloride as the only hydrogen atom source, the initially formed compound I analogue can be observed as a transient because of the increased difficulty of hydrogen atom abstraction. The further increase in difficulty of ^{2}H abstraction from methylene-d_2 chloride explains the extended lifetime of the oxoferryl porphyrin cation radical and the decay process which does not involve the oxoferryl species as an intermediate. THF and DMF are potentially reductants by electron transfer (from nonbonding electrons of oxygen and nitrogen)[31] as well as hydrogen atom abstraction; however, preliminary work on oxidation of the chloro complex of the (2,4,6-trimethoxyphenyl-substituted porphinato)iron (TPP(2,4,6-OCH$_3$)FeCl) in DMF and DMF-d_7 suggests that hydrogen atom abstraction is involved in reduction by these solvents as well. In DMF, oxidation of the iron porphyrin by mCPBA generates a green complex having an electronic spectrum consistent with an oxoferryl porphyrin cation radical which decays within 2 min to an oxoferryl complex[32] (Figure 8). Oxidation in DMF-d_7 extends the lifetime of the transient to permit acquisition of an ^{1}H NMR spectrum in which resonances corresponding to pyrrole β-protons and phenyl meta protons can

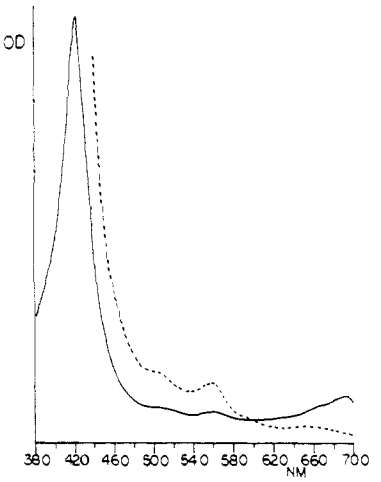

Figure 8. Time dependence of the UV–vis spectrum obtained on oxidation of TPP(2,4,6-OCH$_3$)FeCl in DMF: (—) immediately after addition of mCPBA; (---) after ~2 min.

be observed in the appropriate regions (−13 and 40 ppm, respectively). The existence of an observable oxoferryl porphyrin cation radical in DMF is in accord with decreased reactivity expected for the two-electron oxidation product having the more basic porphyrin ligand and the increased lifetime of the two-electron oxidized complex in perdeuteriated DMF can be attributed to the increased difficulty of ^{2}H abstraction. In the generation of the oxoferryl complex from the chloro (porphinato)iron(III), the ferryl oxo ligand must be derived from the mCPBA oxidant. The parallel chemistry of the chloro and hydroxo (porphinato)iron starting complexes suggests that in the oxidation of TPP(2,6-Cl)FeOH, the hydroxo ligand does not play a role in the redox chemistry other than to effect the stability of the initially produced oxoferryl porphyrin cation radical species. The following reaction scheme leading to the oxoferryl complex may be proposed

$$\text{PFeOH} + \text{mCPBA} \rightarrow [\text{PFe}^{IV}{=}\text{O}]^+ \text{OH}^- + \text{H–Y} \rightarrow \text{PFe}^{IV}{=}\text{O} + \text{H}_2\text{O} + \text{Y}^\cdot$$

where P represents the porphyrinate ligand and H–Y represents solvent or other potential hydrogen atom source in the reaction medium (e.g., ethanol preservative in reagent grade methylene chloride). The reactivity of [Fe^{IV}=O]$^+$ toward reduction by hydrogen abstraction has been demonstrated in a recent report[30] of the reduction of [(TMP)Fe^{IV}=O]$^+$ in the presence of *tert*-butyl hydroperoxide via hydrogen abstraction from the hydroperoxide.

Experimental Section

UV–vis spectra were recorded on a Cary 19 spectrophotometer and ^{1}H NMR spectra on a Bruker AC 200 spectrometer at 200 MHz in DMF-d_7.

The Raman spectra were recorded on a Coderg double monochromator with a spectral slit width of 5 cm^{-1}; the frequency accuracy was ±1 cm^{-1}. A homemade cryostat allowed the temperature of the solution to be kept at −50 °C.

Mössbauer spectra were accumulated with a standard apparatus in the constant-acceleration mode containing a ^{57}Co/Rh (ca. 1.8 GBq) source. Isomer shifts are given with respect to α Fe at room temperature. Experimental spectra were analyzed by a least-squares-fit procedure with use of Lorentzian lines.

Reagents. Tetrahydrofuran was distilled under nitrogen from lithium aluminum hydride, and dimethylformamide was distilled under reduced pressure from 3A molecular sieves. Reagent grade *m*-chloroperoxybenzoic acid (Aldrich) and 1-methylimidazole (Aldrich) were used as received. The porphyrin free base, TPP(2,6-Cl)H$_2$,[33] and its ^{56}Fe complex[34] were prepared according to published methods. To prepare the ^{57}Fe-enriched complex for Mössbauer spectrometry, ^{57}Fe powder (20 mg)

(30) Traylor, T. G.; Xu, F. *J. Am. Chem. Soc.* **1987**, *109*, 6201.
(31) Guengerich, F. P.; MacDonald, T. L. *Acc. Chem. Res.* **1984**, *17*, 9.
(32) The DMF adduct of TPP(2,4,6-OCH$_3$)Fe^{IV}=O has been unambiguously identified by the following data: UV–vis, λ_{max} ($\epsilon \times 10^{-3}$), 422 (118), 558 (6.97), 592 (1.39) nm; Mössbauer, δ 0.10 mm s^{-1}, ΔE_q = 1.91 mm s^{-1}, Γ = 0.59 mm s^{-1}; ^{1}H NMR (200 MHz, DMF-d_7, −40 °C), 13.8 ppm (py-H); $\nu_{Fe^{IV}=O}$ 828 cm^{-1}.
(33) Hill, C. L.; Williamson, M. M. *J. Chem. Soc., Chem. Commun.* **1985**, 1228.
(34) Adler, A. D.; Longo, F. R.; Kampas, F.; Kim, J. *J. Inorg. Nucl. Chem.* **1970**, *32*, 2443.

was treated under argon with refluxing methanol:HCl (10:1, 5 mL) and, after complete solution, the $^{57}FeCl_2$ was isolated by bulb-to-bulb distillation of solvent. A suspension of porphyrin free base (200 mg) in degassed dimethylformamide (30 mL) was added and the mixture refluxed for 24 h under argon. The dimethylformamide was distilled off in vacuo and the solid residue chromatographed over silica with chloroform eluant, yielding a mixture of chloro and hydroxo (porphinato)iron(III) complexes (90 mg). The pure hydroxo complex was obtained by stirring a methylene chloride solution of the mixture overnight with an equal volume of 2 N potassium hydroxide.

Oxidation of the Hydroxo Complex. The tetrahydrofuran and dimethylformamide adducts of the oxoferryl complex were obtained by oxidation at −60 °C in the appropriate solvent with a 4-fold molar excess of *m*-chloroperoxybenzoic acid. The 1-methylimidazole adduct was prepared by addition of a 10-fold molar excess of 1-methylimidazole to the tetrahydrofuran adduct. Solutions for UV-vis spectroscopy were prepared by mixing appropriately diluted stock solutions in a fused silica UV cuvette in a cryostat in the sample compartment of the spectrophotometer. Samples for laser Raman spectra (1.3×10^{-3} M) were prepared by mixing solutions of the porphyrin complex and oxidant in a fused silica cuvette in a low-temperature bath and transferring the cuvette to the sample compartment. Samples for ^1H NMR were similarly prepared in an NMR tube and transferred to the spectrometer probe. Mössbauer samples (2.4×10^{-3} M) were generated in the sample holder (10 mm × 12 mm o.d. delrin cup) glued to a glass adaptor with a milled end by low-temperature epoxy resin (Oxford Instruments, M5) and frozen by plunging the apparatus into liquid nitrogen. The delrin cup was cut from the joint under liquid nitrogen and transferred to the spectrometer.

Acknowledgment. This work was supported in part by USPHS Grant No. ES 03433 and CNRS(UA424). A.G. was the recipient of a Fogarty Fellowship and thanks the Université Louis Pasteur for its hospitality during the tenure of this fellowship.

Registry No. 1, 115227-09-3; **2**, 115227-10-6; **3**, 115227-11-7; **4**, 115227-12-8; **5**, 115244-47-8; mCPBA, 937-14-4; TPP(2,4,6-OCH_3)FeCl, 53470-05-6; DMF(TPP(2,4,6-OCH_3))Fe(O), 115227-13-9; TPP(2,6-Cl)FeOH, 98715-91-4.

Preparation and Molecular and Electronic Structures of a Diamagnetic Diruthenium(II) Compound, $Ru_2[(p\text{-}CH_3C_6H_4)NNN(p\text{-}CH_3C_6H_4)]_4$

F. A. Cotton* and Mark Matusz

Contribution from the Department of Chemistry and Laboratory for Molecular Structure and Bonding, Texas A&M University, College Station, Texas 77843. *Received January 13, 1988*

Abstract: The title compound, $Ru_2[(tol)NNN(tol)]_4$, where tol = p-$CH_3C_6H_4$, has been prepared and characterized by X-ray crystallography, cyclic voltammetry, and several forms of spectroscopy. The compound is diamagnetic (by NMR) and shows one reversible oxidation (in CH_2Cl_2) at +0.28 V vs Ag/AgCl. The structure of the molecule has two notable features: It is strictly eclipsed, and the Ru–Ru distance is 2.417 (2) Å. Both of these structural features, as well as the diamagnetism, lead to the conclusion that the electron configuration is $\sigma^2\pi^4\delta^2\pi^{*4}$. This is in contrast to the occurrence of $\sigma^2\pi^4\delta^2\pi^{*3}\delta^*$ or $\sigma^2\pi^4\delta^2\pi^{*2}\delta^{*2}$ configurations in $Ru_2(O_2CR)_4$ compounds. The large $\delta^*-\pi^*$ gap in the $Ru_2(RNNNR)_4$ type compound in contrast to the small one in the $Ru_2(O_2CR)_4$ compounds is in accord with previous theoretical work. The title compound crystallizes as $Ru_2[(tol)NNN(tol)]_4 \cdot 3C_6H_5CH_3$ in space group $P2_1/c$ with a = 10.539 (2) Å, b = 17.064 (5) Å, c = 19.856 (5) Å, β = 102.30 (2)°, V = 3489 (2) Å^3, and Z = 2.

The electronic structures of diruthenium compounds of the type $Ru_2(LL)_4^n$, where LL is a three-atom, uninegative, bridging bidentate ligand (e.g., RCO_2^-, o-$PhNC_5H_3N^-$, o-$OC_5H_4N^-$, or $RCONH^-$) and n = 0, 1+, or 2+, have provided interesting challenges to theorists and experimentalists alike.[1] These species have 12, 11, or 10 electrons (for charges of 0, 1+, or 2+, respectively) to be allocated to the orbitals that arise primarily from overlap of metal d orbitals. These will be the σ, π, and δ bonding orbitals, which probably come in that order of increasing energy (though it does not matter here since they are all going to be filled), and their antibonding counterparts. Since the first eight electrons can be assigned to the $\sigma^2\pi^4\delta^2$ configuration, the problems that arise concern the ordering of the δ^*, π^*, and σ^* orbitals and how they are occupied by the remaining four, three, or two electrons. There is no doubt that the σ^* orbital is always well above the other two, but the relative energies of the δ^* and π^* orbitals are not easily predictable nor necessarily the same in all cases.

Three general possibilities need to be considered, viz., (I) $E(\delta^*) \ll E(\pi^*)$, (II) $E(\delta^*) \approx E(\pi^*)$, and (III) $E(\delta^*) \gg E(\pi^*)$. Measured magnetic susceptibilities are highly pertinent to determining the correct order, but are sometimes inconclusive. For example, the presence of three unpaired electrons in an $Ru_2(O_2CR)_4^+$ ion indicates case II, but the presence of two unpaired electrons in an $Ru_2(O_2CR)_4$ compound is compatible with either I or II (though III is ruled out). The interpretation of structural results is generally ambiguous. For $Ru_2(O_2CR)_4^{0,1+,2+}$ compounds the Ru–Ru distances vary only over the narrow range 2.248–2.292 Å, but there are also variations in the axial ligands, the effect of which is unknown.

We report here the preparation and properties, including its structure, of $Ru_2[(tol)NNN(tol)]_4$.[2] We shall show that the properties of this compound lead unambiguously to the conclusion that we are dealing with case III, whereby an overall $\sigma^2\pi^4\delta^2\pi^{*4}$ electron configuration is produced.

Experimental Section

Reactions were carried out under anaerobic conditions in standard Schlenkware. Starting materials, $Ru_2(OAc)_4$[3] and di-p-tolyltriazene,[4]

(1) For background and complete references through 1984, see: (a) Cotton, F. A.; Walton, R. A. *Multiple Bonds Between Metal Atoms*; Wiley: New York, 1982. (b) Cotton, F. A.; Walton, R. A. *Struct. Bonding (Berlin)* **1985**, *62*, 19.

(2) The abbreviation (tol)NNN(tol) is used for the anion $[(p\text{-}CH_3C_6H_4)N{=}N{=}N(p\text{-}(CH_3C_6H_4)]^-$.

(3) Lindsay, A. J.; Wilkinson, G.; Motevalli, M.; Hursthouse, M. B. *J. Chem. Soc., Dalton Trans.* **1985**, 2321.

0002-7863/88/1510-5761$01.50/0